applied sciences

MDPI

Article

Impact of Vanadium Complexes with Tetradentate Schiff Base Ligands on the DPPC and EYL Liposome Membranes: EPR Studies

Dariusz Man [1,*], Barbara Pytel [1] and Marzena Białek [2]

[1] Department of Medical Physics, Institute of Physics, Opole University, Oleska 48, 45-052 Opole, Poland
[2] Department of Chemical Technology and Polymer Chemistry, Faculty of Chemistry, Opole University, Oleska 48, 45-052 Opole, Poland
* Correspondence: dariusz.man@uni.opole.pl

Abstract: This paper investigates the effect of three vanadium complexes with Schiff base-type tetradentate ligands of general formula N,N′-1,2-cyclohexylenebis(3,5-dichlorosalicylideneiminate) (**V1**); $LVCl_2$ (L = N,N′-1,2-cyclohexylenebis(5-chlorosalicylideneiminate) (**V2**); and N,N′-1,3propylenebis (salicylideneiminate) (**V3**) on the fluidity of liposome membranes obtained by the sonication of natural lecithin (EYL) and synthetic lecithin (DPPC). The study was carried out with TEMPO and 16DOXYL spin probes using the EPR technique. The results show that the effect of the complexes on the fluidity of liposomes whose membranes are in the liquid crystalline phase is much stronger as compared to the liposome membranes in the gel phase.

Keywords: EPR; vanadium complexes; spin probes; liposomes

Citation: Man, D.; Pytel, B.; Białek, M. Impact of Vanadium Complexes with Tetradentate Schiff Base Ligands on the DPPC and EYL Liposome Membranes: EPR Studies. *Appl. Sci.* **2023**, *13*, 3272. https://doi.org/10.3390/app13053272

Academic Editor: Przemysław M. Płonka

Received: 7 December 2022
Revised: 17 February 2023
Accepted: 17 February 2023
Published: 3 March 2023

1. Introduction

The vanadium concentration in the Earth's crust is approximately 160 ppm. Due to its properties, it is an element with a wide range of applications in many industries. Vanadium steel is used, among others, in the manufacture of springs, cutting tools, and parts for the aircraft industry. Vanadium compounds are used as catalysts in many chemical processes [1–4], e.g., in the production of sulphuric acid and the synthesis of phthalic and maleic anhydrides. They are extensively studied in polymerization reactions, including the coordination polymerization of ethylene and ethylene/1-olefin copolymerization, ring opening polymerization of lactones, and ring opening metathesis polymerization [5–8]. Vanadium catalysts were applied for the synthesis of ethylene/propylene/diene copolymers (EPDM), which were commercialized as synthetic rubbers and ethylene/cyclic olefin copolymers known under the trade name "APEL", which were developed by Mitsui Chemicals, Inc. [6]. For many years, work has been carried out on the application of vanadium compounds in electrochemical processes [9–12], e.g., for electrical energy storage. The importance of vanadium in highly advanced technologies and the number of vanadium products used in everyday life (e.g., batteries) are constantly increasing. Due to their specific chemical properties, vanadium and its compounds also have a strong effect on living organisms [13]. They inhibit cholesterol synthesis and affect glucose metabolism [14,15], which gives hope for their therapeutic applications [16–18] and use in the treatment of diabetes in humans [19]. However, in addition to their desirable therapeutic effects, vanadium compounds also exhibit highly toxic characteristics [20], with destructive effects on living organisms. Vanadium poisoning can lead to disturbances in lipid synthesis, block the action of some enzymes by binding to –SH groups, and cause changes in the composition of proteins and nucleic acids in the blood. One of the effects of vanadium poisoning is a reduction in cysteine levels in the epidermis, dermis, nails, and hair. Contact of the respiratory tract with vanadium oxides can trigger inflammation of the mucous membranes,

causing changes in alveolar macrophages and leading to a decrease in the body's immunity, which is an important factor in the light of the COVID-19 pandemic. On the other hand, the toxicity of vanadium compounds offers hope for their use in anticancer therapies [21–24], involving the development of a new platinum-free preparation. The anticancer activity of vanadium results from its inhibitory effect on the growth of cancer cells [25–28]. Animal studies indicate strong anti-cancer properties in colorectal malignancies [29,30], soft tissue tumours (e.g., leiomyosarcoma), and the in vitro destruction of HeLa malignant tumour cells [31]. Vanadium is also an important micronutrient. It is present in trace amounts in the human body but affects the normal functioning of the body. Vanadium deficiency can increase the likelihood of atherosclerosis and diabetes, and stunt adolescent growth. The data shows that vanadium plays a significant role in both technology and living systems. Therefore, it seems that the effects of vanadium compounds on biological systems, and in particular the effects of organic compounds on the lipid bilayer acting as the structural core of all biological membranes, should be further investigated.

Liposomes, which are relatively easy to produce in the laboratory, are a good model for the lipid bilayer of natural biological membranes. The production of liposomes often involves natural and synthetic lecithin [32–34]. The use of the electron paramagnetic resonance (EPR) technique with spin probes makes it possible to track the changes that occur in the membrane across its cross-section under the influence of various physical or chemical stimuli [35–38].

The purpose of this work is to expand on the research presented in a previous publication [39] that concerned the effect of vanadium compounds (Vanadium(IV)-Oxy Acetylacetonate and Vanadium(III) Acetylacetonate) on DPPC lecithin model membranes. In this work, studies were carried out on the effect of large molecules—three vanadium complexes of different structures—on the structural properties of membranes obtained by sonication of DPPC and EYL lecithin. To date, the influence of these compounds has not been studied in terms of their effect on membranes, in particular on liposome membranes serving as a good model of biological membranes. At physiological temperatures, the lipid bilayer of DPPC liposomes is in the gel phase, while the lipid bilayer of EYL liposomes is in the liquid crystalline phase. The diffusion of vanadium complexes into the centre of the bilayer is likely to be more difficult in the case of DPPC membranes as compared to EYL membranes in the liquid crystalline phase. As EYL and DPPC membranes are very similar (identical in the surface layer), EPR studies using the appropriate spin probes allow for the comparison of the effect of the complexes on the fluidity of the membranes in both phases.

Three vanadium complexes with Schiff base-type tetradentate ligands were selected for this study. Schiff bases containing an azomethine (-HC=N-) or imine (>C=N-) group are some of the most important classes of organic ligands for transition metal complexes because they are able to stabilize many metals in various oxidation states [7,8]. Their structure can be easily changed to modify the electronic and steric environment around the metal, and thus modify the performance of the synthesized complexes. The studied complexes of general formula N,N′-1,2-cyclohexylenebis(3,5-dichlorosalicylideneiminate) (**V1**); $LVCl_2$ (L = N,N′-1,2-cyclohexylenebis(5-chlorosalicylideneiminate) (**V2**); N,N′-1,3-propylenebis (salicylideneiminate) (**V3**) are shown in Figure 1. As can be seen, complexes **V1** and **V2** have a similar molecular structure, differing only in substituent (Cl or H) at position 3 on the aromatic rings. Complex **V3** has a slightly different structure. It contains a propylene bridge between nitrogen atoms instead of a cyclohexylene linker, and it has unsubstituted aromatic rings. The studied vanadium complexes, upon activation with an appropriate organoaluminium compound, were previously used in the polymerization of olefins (ethylene and 1-octene) [40–42]. It was demonstrated that structural changes of the tetradentate Schiff base ligand in the complex (both the type of bridge and the type of substituent on the aryl rings) affect the activity of the catalytic system in ethylene polymerization. The presence of the cyclohexylene bridge and the electron-withdrawing group on the phenolate rings proved beneficial.

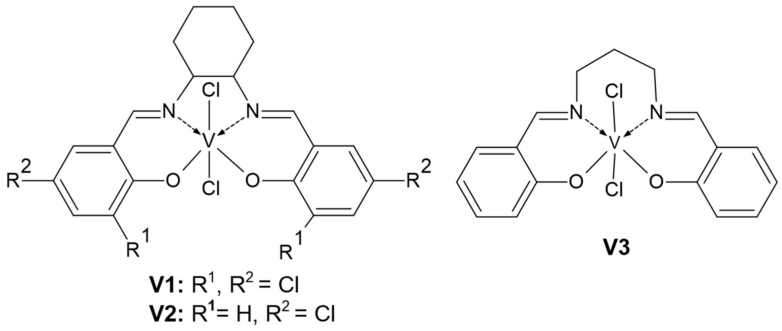

Figure 1. Structure of vanadium complexes.

2. Materials and Methods

2.1. Spin Probes and Lecithin

The spin probes used in the work (Figure 2), 2-ethyl-2-(15-methoxy-15-oxopentadecyl) -4,4-dimethyl-3-oxazolidinyloxy (16-DOXYL-stearic) acid methyl ester and 2, 2,6,6-Tetramethylpiperidine-1-oxyl (TEMPO), as well as synthetic dipalmitoylphosphatidylcholine (DPPC) lecithin and L-α-Phosphatidylcholine (EYL) egg yolk lecithin (Figure 3), were purchased from Merck (Poznań, Poland).

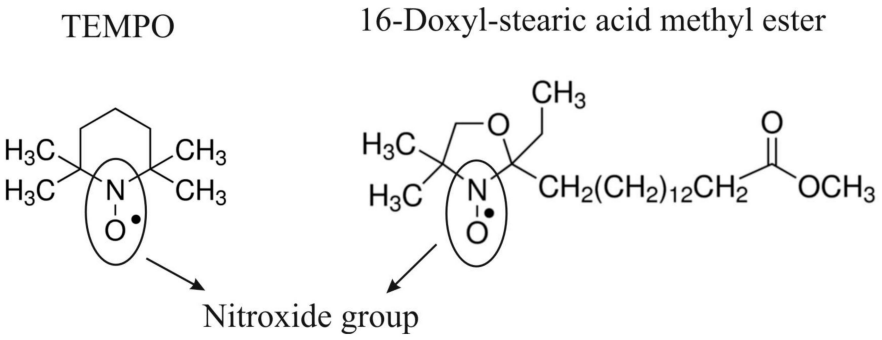

Figure 2. Chemical structure of the spin probes TEMPO (2,2,6,6-tetramethylpiperidine-1-oxyl) and 16-DOXYL(2-ethyl-2-(15-methoxy-15-oxopentadecyl)-4,4-dimethyl-3-oxazolidinyloxy) stearic acid methyl ester; the position of the spin-active nitroxyl groups was indicated.

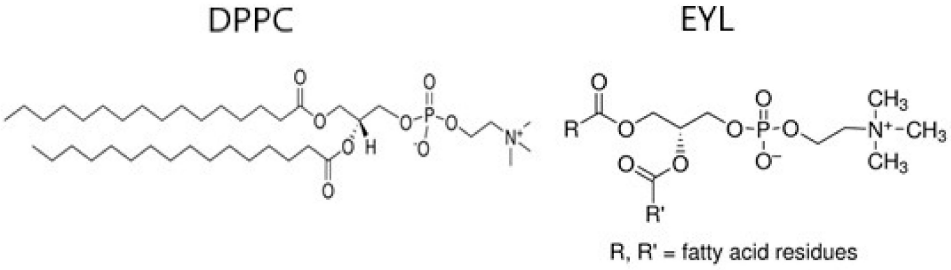

Figure 3. Chemical structure of lecithin: DPPC (1,2-dipalmitoyl-*sn*-glycero-3-phosphocholine) and EYL (L-α-Lecithin, Azolectin, 3-sn-Phosphatidylcholine, PC, 1,2-Diacyl-sn-glycero-3-phosphocholine).

2.2. Vanadium Complexes

The vanadium complexes (Figure 1) **V1** (N,N′-1,2-cyclohexylenebis(3,5-dichlorosalicylideneiminato)vanadium dichloride, molecular formula $C_{20}H_{16}Cl_6N_2O_2V$), **V2** (N,N′-1,2-cyclohexylenebis(5-chlorosalicylideneiminato)vanadium dichloride, molecular formula $C_{20}H_{18}Cl_4N_2O_2V$) and **V3** (N,N′-1,3-propylenebis (salicylideneiminato)vanadium dichloride, molecular formula $C_{17}H_{16}Cl_2N_2O_2V$) were prepared according to the procedure described in the literature [40–42]. The appropriate ligand was dissolved in dichloromethane,

and then a solution of VCl_4 in hexane was introduced dropwise at the molar ratio of 1:1 in relation to ligand. The reaction was carried out overnight at room temperature. Then, the reaction mixture was concentrated. The complex was separated by filtration, washed with dichloromethane and hexane, and dried under vacuum. Syntheses were carried out under argon atmosphere. The solvents were dried by standard methods.

2.3. Liposom Membranes

Monolayer liposomes were produced by the sonication of DPPC and EYL in distilled water using an ultrasonic disintegrator (UD-20; Techpan, Warszawa, Poland). The sonication time for a single 2 mL sample was 6 min. The process consisted of 6 cycles involving 30 s of sonication and 30 s of cooling. The concentration of lecithin in the sample was 40 µM. After sonication, the aqueous dispersion of the liposomes was divided into two sections containing TEMPO and 16DOXYL spin probes, respectively. The concentration of the probes relative to lecithin (DPPC or EYL) was 500 ppm. The samples containing liposomes and probes were shaken for 10 min and allowed to stabilize for 15 min. The liposomes were supplemented with the appropriate vanadium complex, shaken again for 5 min, and measured in an EPR spectrometer. EPR measurements were performed at constant temperature (22 °C) using an X-band spectrometer (SE/X28 Wrocław University of Technology). The spectra were recorded with the following instrument settings: time constant—0.3 s, modulation amplitude—0.8×10^{-1} mT, scan time—128 s, and sweep range—8 mT. The process was repeated several times, each time with a higher concentration of the additive. The additive concentrations were measured relative to the lecithin in the sample. The EPR spectra (Figure 4a,b) provide information on the fluidity of the membranes in different regions. The TEMPO probe dissolves in both aqueous and lipid environments, indirectly providing information on the fluidity of the surface layer acting as a barrier to the penetration of the lipid environment. The 16DOXYL probe located in the centre of the lipid bilayer provides information on the fluidity of the inner part of the membrane (Figure 5). The EPR spectrum of the TEMPO probe was used to calculate the spectroscopic partition parameter (F) showing how the probe is split between the membrane and its environment. F is defined as the ratio of the amplitudes of the high-field line in the EPR spectrum of the probe dissolved in water (P) to the amplitude of the low-field line (H) of the probe dissolved in the lipid environment (Figure 4a). The F value is related to the fluidity of the membrane surface layer [38,43]. The spectrum of the 16-DOXYL probe was used to determine the τ parameter. Its value depends on the degree of fluidity of the membrane in the middle layer, and it increases with the rise of stiffness (ordering) of the probe environment [38,44,45]. For an isotropic environment, τ is the probe rotational correlation time (Figure 4b). The relative measurement errors were as follows: 2.5% for the F parameter and 3% for the τ parameter.

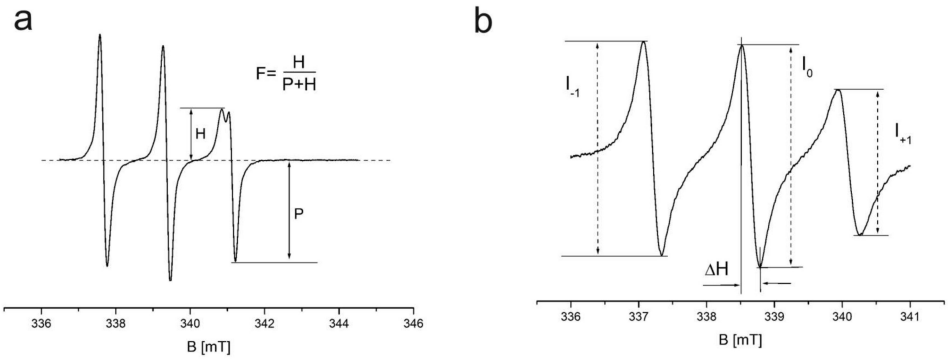

Figure 4. ESR spectra of spin probes placed in the liposome membrane. (**a**) TEMPO probe and spectroscopic partition parameter (*F*); (**b**) 16-DOXYLstearicacid methyl ester probe and rotational correlation time parameter (*τ*); $\tau = 5.95 \cdot \Delta H(I_0/I + 1)^{1/2} + (I_0/I{-}1)^{1/2} - 2)10^{-10}$ [s].

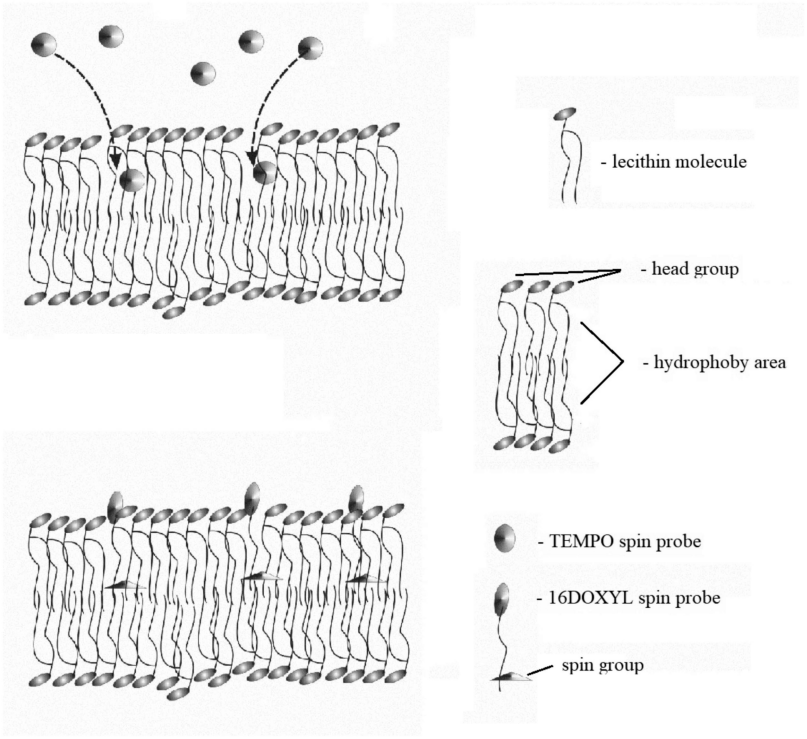

Figure 5. The location of probes in the lipid bilayer of liposome.

2.4. Computer-Based Model

For mathematical analysis and visualization of the processes that occur in the surface layer of the membrane, a computer model was developed. The model consists of N (value declared as a simulation parameter) electric dipoles that can move on the surface of the membrane and rotate around its own axis perpendicular to the surface of the membrane. The mobility of the dipoles is declared as a simulation parameter. The energy of the surface layer of the membrane is described by the Hamiltonian:

$$H = \sum_{(i)} \frac{p_i^2}{2m} + \sum_{(i)} \frac{L_i^2}{2I} + \sum_{(i<j)} U_{ij} \tag{1}$$

where m—dipole mass, I—moment of inertia, p_i—dipole momentum, and L_i—dipole angular momentum. The first two terms of the equation refer to the kinetic energy of the dipoles associated with translational and rotational motion. The third term of the equation represents the Coulomb and Lennard-Jones interactions between all dipoles:

$$U_{ij} = \frac{e^2}{4\pi\varepsilon_0\varepsilon_r}\left(\frac{1}{\left|\vec{d}_{ij}+\vec{a}_j-\vec{a}_i\right|} - \frac{1}{\left|\vec{d}_{ij}-\vec{a}_j-\vec{a}_i\right|} + \frac{1}{\left|\vec{d}_{ij}-\vec{a}_j+\vec{a}_i\right|} - \frac{1}{\left|\vec{d}_{ij}+\vec{a}_j+\vec{a}_i\right|}\right) + 4\varepsilon\left[\left(\frac{\sigma}{\left|\vec{d}_{ij}\right|}\right)^{12} - \left(\frac{\sigma}{\left|\vec{d}_{ij}\right|}\right)^{6}\right] \tag{2}$$

The meanings of vectors a and d are described in Figure 6.

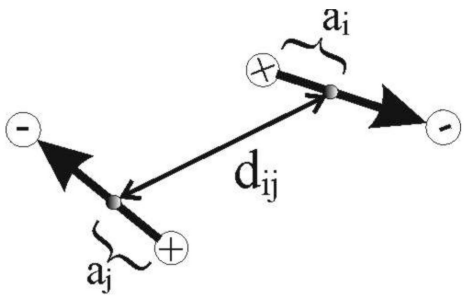

Figure 6. Parameterization of dipoles.

The model represents a system of dipoles arranged on a round cork floating in a sea of lipids. The system defined in this way has three degrees of freedom. Two of them relate to the translational motion of the dipole, and one corresponds to its rotation. In real lipid membranes, the polar head group (dipoles) forming the surface layer is anchored on hydrocarbon chains that limit their mobility. The presence of these chains also prevents the heads (dipoles) from getting closer to one another. In the mathematical model, this property is represented by the Lennard-Jones potential. The degree of this limitation is set by the depth of the potential described by the ε parameter. Increasing the value of ε makes the simulated membrane stiffer. The σ parameter determines the average distance between the dipoles. It is determined on the basis of literature data. In the case of EYL and DPPC lecithin, it is about 1 nm. The dynamics of the chains connected to the heads indirectly affects the dynamics of the heads. However, this is not a strict correlation because the mobility of the polar head group is significantly lower than the mobility of the hydrocarbon chains. The rotation time of the polar heads is around 10^{-9} s, while the oscillation times of the chains are estimated at 10^{-14} s. The model assumes that this effect is purely stochastic and uncorrelated, which is a simplification compared to the real membrane.

The simulation algorithm is based on the Monte Carlo Metropolis algorithm in the statistical canonical ensemble. In this algorithm, the part coming from the kinetic energy is calculated analytically, while the part coming from the potential energy is the basis for the simulation and determines the probability (w) of accepting a randomly selected new state.

$$w = \exp\left(-\frac{\Delta E_p}{k_B T}\right) \tag{3}$$

where k_B is the Boltzmann constant, T is the temperature, and ΔEp is the change in the potential energy of the system between the previous state and the new state. If the new state leads to a lower energy of the system ($-\Delta$Ep), the $\boldsymbol{w}$ parameter is greater than 1. This means that the state is always accepted. It represents the current state of the system. When the energy of the system increases, w takes values from 0 to 1 and determines the probability of accepting the new state. In the equilibrium state, the temperature is related to the kinetic energy of the dipoles. As the formula shows, an increase in temperature causes the exponent to decrease so w tends towards unity. This increases the probability of accepting states with higher potential energy. A new state of the system is created by changing the position and orientation of a randomly selected dipole according to the Gaussian distribution.

The aim of the simulation is to show the changes that occur in the surface layer of the membrane, depending on the degree of its fluidity. In the gel phase, polar heads have very limited mobility. They form an ordered structure (pseudo-crystalline), which virtually closes the entrance into the lipid bilayer. The increase in fluidity results in the increase in the mobility of membrane-building lipid molecules. Therefore, voids are expected to form in the surface region of the membrane. In the simulation, this is illustrated as the formation of free spaces between the dipoles representing the polar heads. The degree of fluidity of the membrane in the simulation is regulated by parameters related to the translational motion of the dipoles and the rotational speed of the dipoles.

3. Results

This section is divided into further subsections. It provides a concise and precise description and interpretation of the experimental results and the experimental conclusions.

3.1. EPR Spectra of Vanadium Complexes

The vanadium complexes (**V1**, **V2**, and **V3**) were dissolved in dimethylformamide (DMF) and introduced into glass capillaries. The capillaries were successively inserted into the chamber of the EPR spectrometer. The measurements were carried out at 22 °C. The spectral 8 lines obtained in the study are shown in Figure 7. The spectral parameters and g values corresponding to the lines are listed in Table 1. The width of the sweep window was 100 mT, and the sweep time was set at 256 s. The EPR spectra of the complexes are very similar and typical for vanadium compounds [4,46], except for an additional line at g = 1.994 in the spectral image of the **V1** complex. The g value of this line shows that there is a certain pool of spins corresponding to weakly bound electrons.

Table 1. Spectroscopic parameters of EPR spectral lines of vanadium complexes.

	V3			**V1**			**V2**		
Line No.	**dH [mT]**	**Centre [mT]**	**g**	**dH [mT]**	**Centre [mT]**	**g**	**dH [mT]**	**Centre [mT]**	**g**
1	1.496	306.146	2.249766	1.554	306.145	2.249773	1.902	306.225	2.249186
2	1.369	316.382	2.176979	1.353	316.406	2.176814	1.647	316.484	2.176277
3	1.211	326.947	2.106632	1.245	326.963	2.106529	1.47	327.022	2.106149
4	1.241	337.945	2.038074	1.232	337.97	2.037923	1.484	338.027	2.03758
5	1.393	349.364	1.971459	1.365	349.268	1.972001	1.669	349.405	1.971228
6	1.634	361.147	1.907137	1.633	361.135	1.907201	1.997	361.156	1.90709
7	1.925	373.247	1.845311	1.932	373.241	1.845341	2.408	373.186	1.845613
8	2.359	385.759	1.785459	2.417	385.736	1.785566	2.951	385.683	1.785811
0				2.842	345.424	1.993946			

3.2. Effect of Vanadium Complexes on EYL Liposome Membranes

3.2.1. TEMPO Probe

Figure 8 shows F for the TEMPO probe as a function of the concentration of **V2** and **V1** additives. To illustrate the additive-induced changes more clearly, changes in F were normalized to 1, where F_0 is the value for liposomes without an additive and F is the partition parameter for a given additive concentration. Values above 1 mean that more probe from the water-lipid dispersion passes into the membrane, which may indicate an increase in membrane fluidity in its surface layer [32,33,38,43]. The data presented in Figure 6 show that both vanadium complexes (**V1** and **V2**) significantly increase membrane fluidity. **V1** had a particularly active effect on the surface layer of the liposomes. It caused a strong, monotonic increase in F/F_0 with increasing concentration, except for the concentration region of 2–3%, where a small plateau (possibly related to the phase transition) was observed. For membranes with **V2**, a monotonic increase in F/F_0 was also observed. However, it was less dynamic and without a plateau.

3.2.2. 16DOXYL Probe

Figure 9 shows the rotational correlation time parameter (τ) for the 16DOXYL probe as a function of the concentration of **V1**, **V2**, and **V3** additives. Similar to Figure 8, to illustrate additive-induced changes more clearly, changes in τ were normalized to 1, where τ_0 is the value for liposomes without additive and τ is the parameter value for a given additive concentration. A τ/τ_0 above 1 shows that the probe slowed down the rotation, which may indicate a decrease in membrane fluidity in the central part of the bilayer. The data

presented in Figure 8 shows that the vanadium complexes significantly increase the fluidity of the membrane in its central region. This process was monotonic in the concentration range of 0% to 2–3%, causing a change in the parameter of 20% for **V3**, 25% for **V1**, and 30% for **V2**. Above these concentration values, the curve flattened, indicating a saturation of the fluidity process.

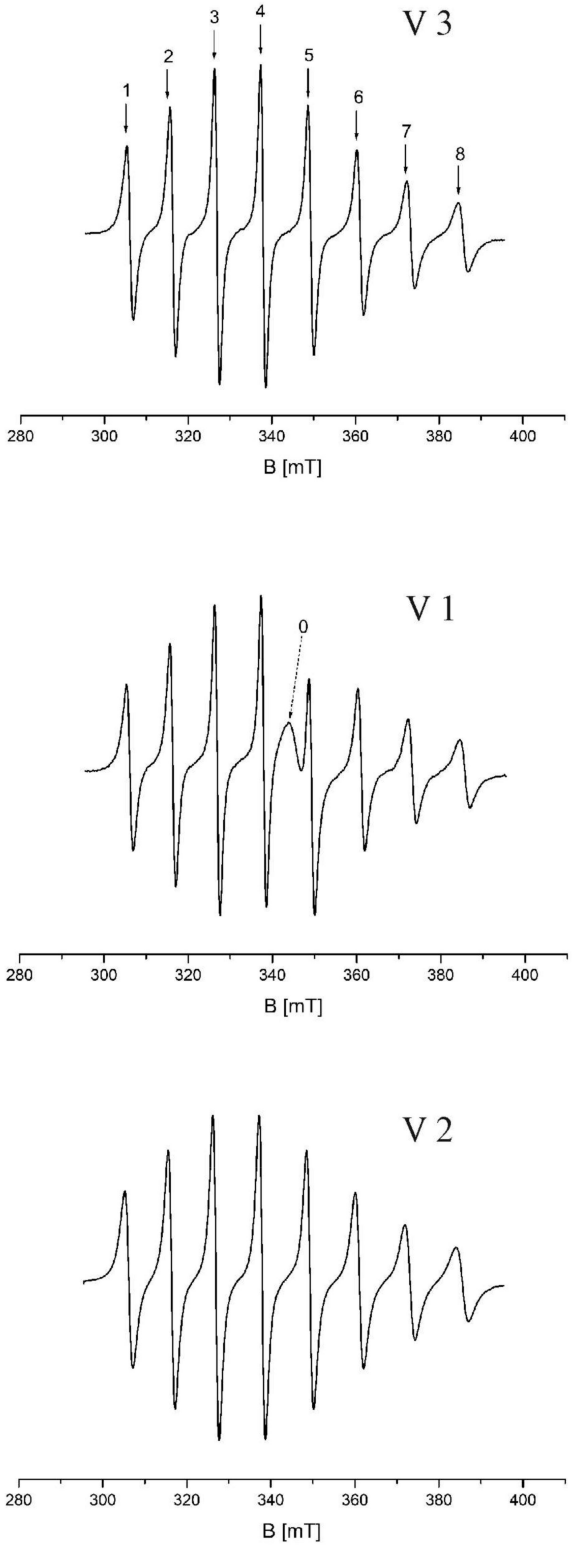

Figure 7. Spectroscopic lines of vanadium complexes (**V3**, **V1**, **V2**) dissolved in DMF.

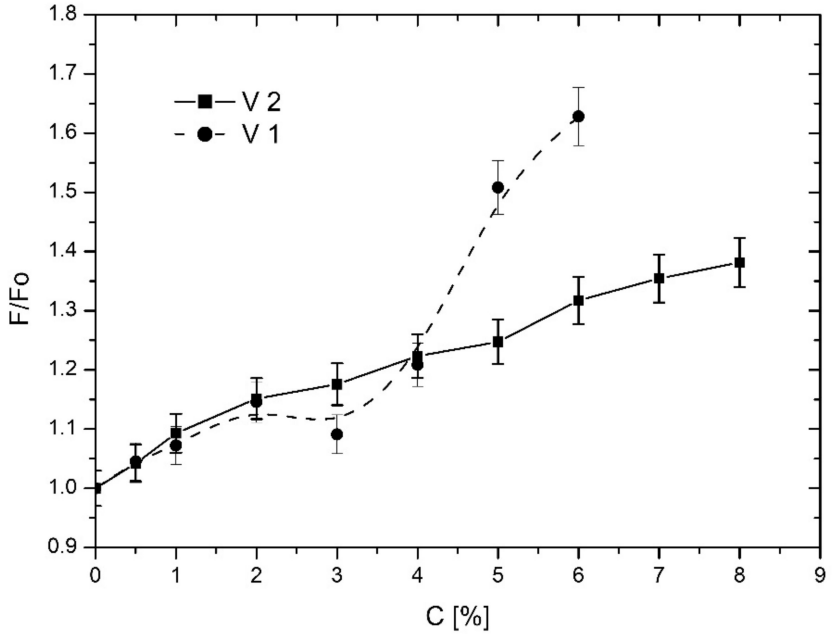

Figure 8. Effect of the vanadium complexes on the water–EYL liposome membrane interface, as featured by EPR measurements for the TEMPO spin label. F/F_0 represents the relative partition parameter for spin label; values greater than 1 and less than 1 indicate the increase and decrease in fluidity, respectively.

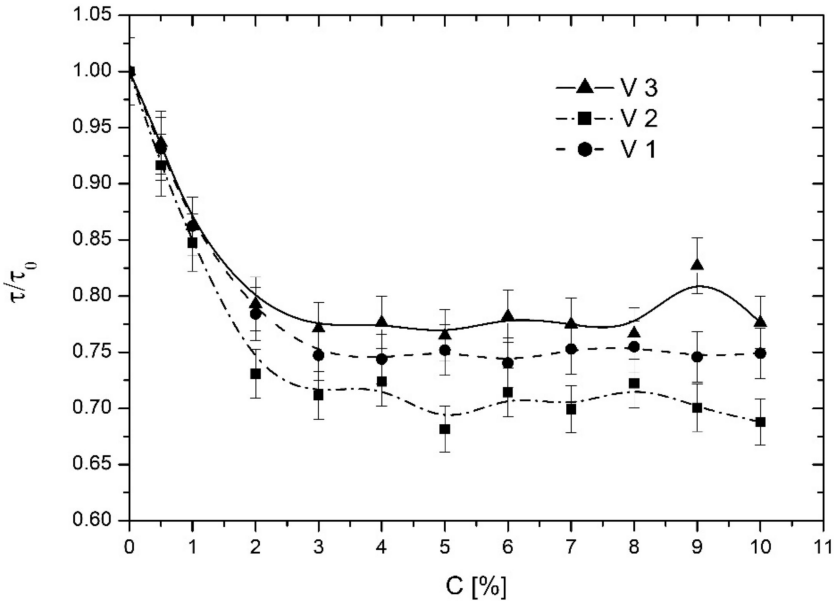

Figure 9. Effect of the vanadium complexes on the central part of the liposome EYL membrane as featured by EPR measurements involving the 16-DOXYL spin label; τ/τ_0 represents the relative rotational correlation time parameter for spin label; values less than 1 and greater than 1 indicate increase and the decrease in fluidity, respectively.

3.3. Effect of Vanadium Complexes on DPPC Liposome Membranes

3.3.1. TEMPO Probe

Figure 10 shows F for the TEMPO probe placed in an aqueous dispersion of liposomes formed from DPPC as a function of the concentration of **V1**, **V2**, and **V3** additives. As in the previous cases, the changes in the partition parameter of the TEMPO probe are presented in relative units normalized to 1. **V2** had virtually no effect on the changes in

F. Only a slight tendency towards stiffening of the membrane surface layer was observed, as evidenced by a slight decrease in F/F_0. The changes were stronger for **V3** and **V1**. For **V1** in the 0–2% concentration range, there was a decrease in F/F_0 of about 15%, to 0.85. Above 2% concentration, the changes of the parameter stabilized as it fluctuated around 0.85. A similar effect was observed for **V3**. However, the greatest decrease in F/F_0 was achieved for the 3% additive concentration. Again, above this concentration, the changes of the parameter stabilized, and it fluctuated around 0.85. In general, it can be concluded that the effect of the complexes on the changes in F was much weaker for DPPC membranes than for EYL membranes, and surprisingly, it slightly stiffened the liposome membranes.

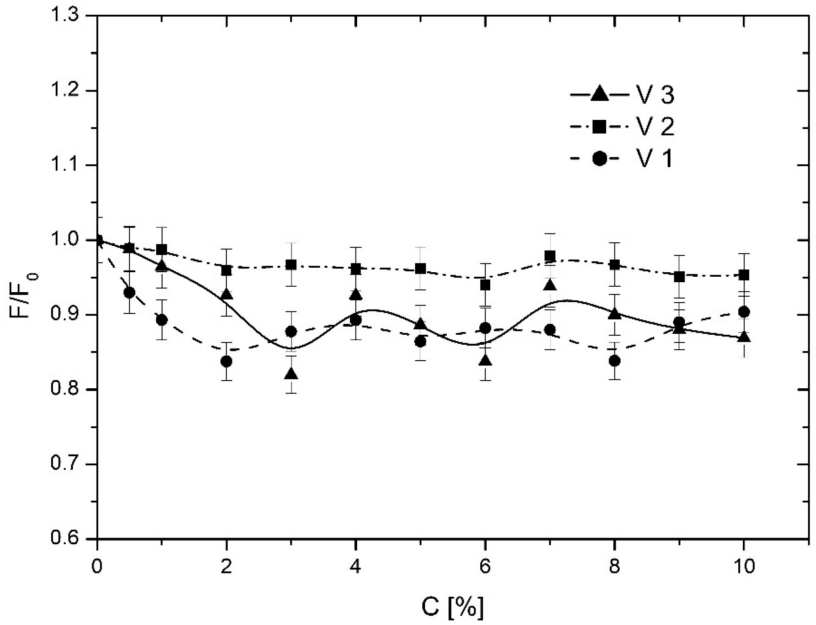

Figure 10. Effect of the vanadium complexes on the water–DPPC liposome membrane interface, as featured by EPR measurements for the TEMPO spin label. F/F_0 represents the relative partition parameter for spin label; values greater than 1 and less than 1 indicate the increase and decrease in fluidity, respectively.

3.3.2. 16DOXYL Probe

Figure 11 shows τ for the 16DOXYL probe placed in an aqueous dispersion of liposomes formed from DPPC as a function of the concentration of **V1**, **V2**, and **V3** additives. As in the previous cases, the changes in the rotational correlation time parameter of the TEMPO probe are presented in relative units normalized to 1. The data presented in Figure 8 shows that **V2** and **V1** slightly fluidized the central part of the lipid bilayer, while **V3** stiffened this region. Again, the changes induced by the vanadium complexes were significantly smaller than for the EYL liposome membranes. Only **V3** caused a slightly larger change in τ/τ_0 of about 10–15% for the 5–7% additive concentration range. The occurrence of an extreme at a value of about 6% for this compound is also surprising. This may indicate that the kinetics of **V3** dissolution in the lipid environment of the membrane is complex. For **V2** and **V1**, no effect on τ/τ_0 was observed up to a concentration of 7%. Above this concentration, **V2** caused a slight change in the parameter (<10%), which may indicate a slight fluidization of the membrane in its central region.

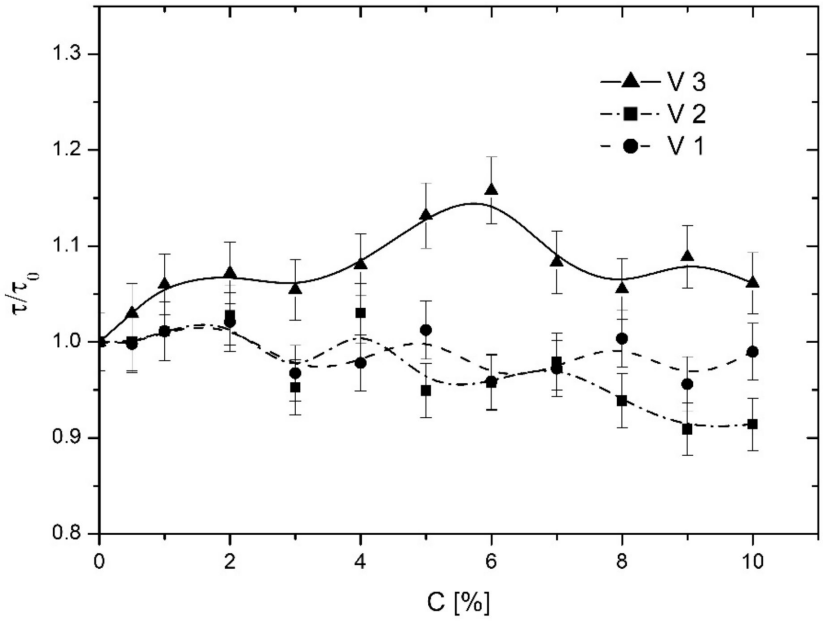

Figure 11. Effect of the vanadium complexes on the central part of the liposome DPPC membrane, as featured by EPR measurements involving the 16-DOXYL spin label; τ/τ_0 represents the relative rotational correlation time parameter for spin label; values less than 1 and greater than 1 indicate the increase and decrease in fluidity, respectively.

4. Conclusions

The conclusions from the study are as follows: The vanadium complexes have a stronger effect on the fluidity of the membranes of EYL liposomes compared to DPPC liposomes. This is because the membranes of EYL liposomes at 22 °C (temperature of the experiment) were in the liquid crystalline phase, while the membranes of DPPC liposomes were in the gel phase. As reported in [38], the surface part of the lipid bilayer of membranes located in the liquid crystalline phase has gaps of different sizes (Figure 12), through which molecules of the vanadium complexes can diffuse deep into the lipid bilayer. In addition, the hydrocarbon chains of the membrane-building lipids are more mobile in the liquid crystalline phase than in the gel phase, which favours the dissolution of the additives. The relationship is clearly illustrated by the graphs shown in Figures 7 and 9. In the liquid crystalline phase, the changes induced by the additives were evident, changing τ/τ_0 in the 25–35% range. In the gel phase, **V2** and **V1** did not induce any changes in τ/τ_0 at low concentrations. The negligible effect of the vanadium complexes on the fluidity of the DPPC membranes as compared to the EYL membranes is due to the compact structure of the polar head groups in the gel phase (Figure 12). Computer simulations of this layer [38] show that a number of defects can be formed when the membrane is in the liquid crystalline phase. Given the size and number of such gaps (defects) in the compact structure of the membrane surface, hydrophobic molecules were able to penetrate its interior. The greater influence on the membrane fluidity of the DPPC liposomes of **V3** (Figure 11) is due to its different molecular structure as compared to **V2** and **V1** (Figure 3). It was probably easier for it to pass through the polar head group's region and penetrate into the central part of the lipid bilayer. The exceptionally strong effect of **V1** on the surface layer of EYL liposomes (Figure 8) is due to the presence of a certain pool of relatively weakly bound electrons in the structure of the molecule that can easily interact with the surface region of the membrane. This is shown in Figure 7. For **V1**, the spectral line marked "0" corresponds approximately to the value of g = 2 (Table 1), which is typical for weakly bound electrons. The EPR spectra of **V3** and **V2** did not have the line.

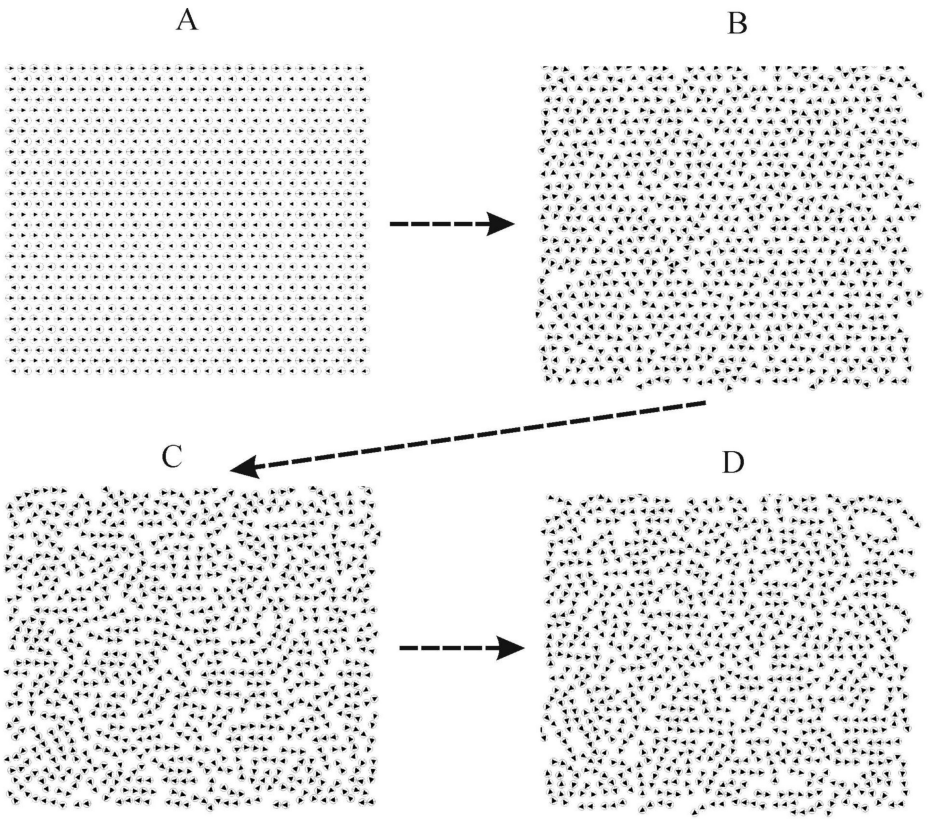

Figure 12. Images of bitmaps obtained in the process of simulating the surface layer of lipid membranes. The surface layer in the simulation is represented by a system of 30 × 30 electric dipoles. The dipole dimensions were set at 0.5 nm, in accordance with the dimensions given in [47] for phosphatidylcholine. Bitmaps: (**A**)—gel phase (DPPC liposomes), (**B**,**C**)—transition state between the gel phase and the liquid crystal phase, (**D**)—liquid crystalline phase (EYL liposomes).

The effect of the vanadium complexes on the fluidity of the liposome membranes strongly depends on the phase. There are two different effects observed for the same complexes: a strong increase in the fluidity of the membranes that were in the liquid crystalline phase and a slight decrease in the fluidity of the membranes that were in the gel phase. Furthermore, the effects of the complexes in the liquid crystalline phase are several times stronger than in the gel phase, which is probably due to the gaps in the polar head group layer. This may have important implications for further research in some areas of medicine and pharmacy (controlled drug release, drug absorption by cells), as well as in the areas of technology involving the transport of active substances across semipermeable membranes. It seems that the critical point here is to precisely control the fluidity of the surface layer of the membranes by controlling the number and size of the gaps.

Author Contributions: Conceptualization, D.M.; methodology, D.M. and M.B.; software, D.M.; validation, D.M., B.P. and M.B.; formal analysis, D.M.; investigation, D.M. and B.P.; resources, D.M.; data curation, D.M. and B.P.; writing—original draft preparation, D.M.; writing—review and editing, D.M. and B.P.; visualization, B.P.; supervision, D.M. All authors have read and agreed to the published version of the manuscript.

Funding: This research received no external funding.

Institutional Review Board Statement: Not applicable.

Informed Consent Statement: Not applicable.

Data Availability Statement: Not applicable.

Conflicts of Interest: The authors declare no conflict of interest.

References

1. Bihun-Kisiel, A.; Ochędzan-Siodłak, W. Vanadium catalysts for ethylene-norbornene. *Copolym. Polim.* **2020**, *65*, 757–770. [CrossRef]
2. Ochędzan-Siodłak, W.; Bihun, A.; Olszowy, A.; Rajfur, M.; Jesionowski, T.; Siwińska-Stefańska, K. Ethylene polymerization using vanadium catalyst supported on silica modified by pyridinium ionic liquid. *Polym. Int.* **2016**, *65*, 1089–1097. [CrossRef]
3. Mirchev, N.; Lazarova, D.; Georgieva, M.; Petrova, M.; Tachev, D.; Avdeev, G. Preparation of Cu/ZrW_2O_8 structures by chemical deposition from formaldehyde-free solution. *Trans. IMF* **2020**, *100*, 18–24. [CrossRef]
4. Groch, P.; Dziubek, K.; Czaja, K.; Białek, M.; Man, D. Tri-alkenyl polyhedral oligomeric silsesquioxanes as comonomers and active center modifiers in ethylene copolymerization catalyzed by bis(phenoxyimine) Ti, Zr, V and V salen-type complexes. *Appl. Catal. A Gen.* **2018**, *567*, 122–131. [CrossRef]
5. Ishikura, H.; Neven, R.; Lange, T.; Galetova, A.; Blom, B.; Romano, D. Developments in vanadium-catalysed polymerisation reactions: A review. *Inorg. Chim. Acta* **2021**, *515*, 120047. [CrossRef]
6. Nomura, K.; Zhang, S. Design of Vanadium Complex Catalysts for Precise Olefin Polymerization. *Chem. Rev.* **2011**, *111*, 2342–2362. [CrossRef]
7. Cozzi, P.G. Metal–Salen Schiff base complexes in catalysis: Practical aspects. *Chem. Soc. Rev.* **2004**, *33*, 410–421. [CrossRef]
8. Liu, X.; Hamon, J.-R. Recent developments in penta-, hexa- and heptadentate Schiff base ligands and their metal complexes. *Coord. Chem. Rev.* **2019**, *389*, 94–118. [CrossRef]
9. Li, L.; Kim, S.; Wang, W.; Vijayakumar, M.; Nie, Z.; Chen, B.; Zhang, J.; Xia, G.; Hu, J.; Graff, G.; et al. A stable vanadium redoxflow battery with high energy density for large-scale energy storage. *Adv. Energy Mater.* **2011**, *1*, 394–400. [CrossRef]
10. Rahman, F.; Skyllas-Kazacos, M. Vanadium redox battery: Positive half-cell electrolyte studies. *J. Power Sources* **2009**, *189*, 1212–1219. [CrossRef]
11. Skyllas-Kazacos, M.; Cao, L.; Kazacos, M.; Kausar, N.; Mousa, A. Vanadium electrolyte studies for the vanadium redox battery—A review. *ChemSusChem* **2016**, *9*, 1521–1543. [CrossRef]
12. Sun, C.; Chen, J.; Zhang, H.; Han, X.; Luo, Q. Investigations on transfer of water and vanadium ions across nafion membrane in an operating vanadium redox flow battery. *J. Power Sources* **2010**, *195*, 890–897. [CrossRef]
13. Galloni, P.; Conte, V.; Floris, B. A journey into the electrochemistry of vanadium compounds. *Coord. Chem. Rev.* **2015**, *301–302*, 240–299. [CrossRef]
14. Goldwaser, I.; Qian, S.; Gershonov, E.; Fridkin, M.; Shechter, Y. Organic vanadium chelators potentiate vanadium-evoked glucose metabolism in vitro and in vivo: Establishing criteria for optimal chelators. *Mol. Pharmacol.* **2000**, *58*, 738–746. [CrossRef]
15. Brannick, B.; Kocak, M.; Solomon, S. Vanadium in Glucose Metabolism: Past, Present and Future. *J. Toxicol. Pharm.* **2017**, *1*, 1–011.
16. Heyliger, C.E.; Tahiliani, A.G.; McNeill, J.H. Effect of Vanadate on Elevated Blood Glucose and Depressed Cardiac Performance of Diabetic Rats. *Science* **1985**, *227*, 1474–1477. [CrossRef]
17. Meyerovitch, J.; Backer, J.M.; Kahn, C.R. Hepatic phosphotyrosine phosphatase activity and its alterations in diabetic rats. *J. Clin. Investig.* **1989**, *84*, 976–983. [CrossRef]
18. Yun, J.H.; Park, S.H.; Choi, G.H.; Park, I.J.; Lee, J.H.; Lee, O.H.; Kim, J.H.; Seo, Y.H.; Cho, J.H. Antidiabetic effect of an extract of nutricultured Brassica napus containing vanadium from a Jeju water concentrate. *Food Sci. Biotechnol.* **2018**, *28*, 209–214. [CrossRef]
19. Srivastava, A.K.; Mehdi, M.Z. Insulino-mimetic and anti-diabetic effects of vanadium compounds. *Diabet. Med.* **2005**, *22*, 2–13. [CrossRef]
20. Hao, L.; Zhang, B.; Feng, C.; Zhang, Z.; Lei, Z.; Shimizu, K. Human health risk of vanadium in farmland soils near various vanadium ore mining areas and bioremediation assessment. *Chemosphere* **2021**, *263*, 128246. [CrossRef]
21. Evangelou, A.M. Vanadium in cancer treatment. *Crit. Rev. Oncol. Hematol.* **2002**, *42*, 249–265. [CrossRef] [PubMed]
22. Strianese, M.; Basile, A.; Mazzone, A.; Morello, S.; Turco, M.C.; Pellecchia, C.J. Therapeutic potential of a pyridoxal-based vanadium(IV) complex showing selective cytotoxicity for cancer versus healthy cells. *Cell Physiol.* **2013**, *228*, 2202–2209. [CrossRef] [PubMed]
23. Levina, A.; Lay, P.A. Stabilities and biological activities of vanadium drugs: What is the nature of the active species? *Chem. Asian J.* **2017**, *12*, 1692–1699. [CrossRef] [PubMed]
24. Kioseoglou, E.; Petanidis, S.; Gabriel, C.; Salifoglou, A. The chemistry and biology of vanadium compounds in cancer therapeutics. *Coord. Chem. Rev.* **2015**, *301*, 87–105. [CrossRef]
25. Levina, A.; Pires Vieira, A.; Wijetunga, A.; Kaur, R.; Koehn, J.T.; Cran, D.C.; La, P.A. A Short-Lived but Highly Cytotoxic Vanadium (V) Complex as a Potential Drug Lead for Brain Cancer Treatment by Intratumoral Injections. *Angew. Chem. Int. Ed.* **2020**, *59*, 15834–15838. [CrossRef]
26. Corona-Motolinia, N.D.; Martínez-Valencia, B.; Noriega, L.; Sánchez-Gaytán, B.L.; Méndez-Rojas, M.Á.; Melendez, F.J.; González-Vergara, E. Synthesis, crystal structure, and computational methods of vanadium and copper compounds as potential drugs for cancer treatment. *Molecules* **2020**, *25*, 4679. [CrossRef]
27. Crans, D.C.; Koehn, J.T.; Petry, S.M.; Glover, C.M.; Wijetunga, A.; Kaur, R.; Lay, P.A. Hydrophobicity may enhance membrane affinity and anti-cancer effects of Schiff base vanadium (v) catecholate complexes. *Dalton Trans.* **2019**, *48*, 6383–6395. [CrossRef]

28. Ścibior, A.; Pietrzyk, Ł.; Plewa, Z.; Skiba, A. Vanadium: Risks and possible benefits in the light of a comprehensive overview of its pharmacotoxicological mechanisms and multi-applications with a summary of further research trends. *J. Trace Elem. Med. Biol.* **2020**, *61*, 126508. [CrossRef]
29. Kanna, P.S.; Mahendrakumar, C.B.; Indira, B.N.; Srivastawa, S.; Kalaiselvi, K.; Elayaraja, T.; Chatterjee, M. Chemopreventive effects of vanadium toward 1,2-dimethylhydrazine-induced genotoxicity and preneoplastic lesions in rat colon. *Environ. Mol. Mutagen.* **2004**, *44*, 113–118. [CrossRef]
30. Anupam, B.; Abhijeet, W.; Mehool, A.P.; Malay, C. Vanadium in the detection, prevention and treatment of cancer: The in vivo evidence. *Cancer Lett.* **2010**, *294*, 1–12. [CrossRef]
31. Liasko, R.; Karkabounas, S.; Kabanos, T. Antitumor effects of a Vanadium complex with cysteine on malignant cell lines and tumorbearing Wistar rats. *Met. Ions Biol. Med.* **2000**, *6*, 577–579.
32. Man, D.; Pisarek, I.; Braczkowski, M.; Pytel, B.; Olchawa, R. The impact of humic and fulvic acids on the dynamic properties of liposome membranes: The ESR method. *J. Liposome Res.* **2014**, *24*, 106–112. [CrossRef]
33. Man, D.; Olchawa, R. Two-step impact of Amphotericin B AmB on lipid membranes. ESR experiment and computer simulations. *J. Liposome Res.* **2013**, *23*, 327–335. [CrossRef]
34. Wałęsa, R.; Man, D.; Engel, G.; Siodłak, D.; Kupka, T.; Ptak, T.; Broda, M.A. The Impact of Model Peptides on Structural and Dynamic Properties of Egg Yolk Lecithin Liposomes—Experimental and DFT Studies. *Chem. Biodivers.* **2015**, *12*, 1007–1024. [CrossRef]
35. Pytel, B.; Filipiak, A.; Pisarek, I.; Olchawa, R.; Man, D. Impact of humic acids on EYL liposome membranes: ESR method. *Nukleonika* **2015**, *60*, 455–459. [CrossRef]
36. Dyrda, G.; Boniewska-Bernacka, E.; Man, D.; Barchiewicz, K.; Słota, R. The effect of organic solvents on selected microorganisms and model liposome membrane. *Mol. Biol. Rep.* **2019**, *46*, 3225–3232. [CrossRef]
37. Man, D.; Słota, R.; Kawecka, A.; Engel, G.; Dyrda, G. Liposomes modified by mono- and bis-phthalocyanines: A comprehensive EPR study. *Eur. Phys. J. E* **2017**, *40*, 63. [CrossRef]
38. Man, D.; Olchawa, R. Dynamics of surface of lipid membranes: Theoretical considerations and the ESR experiment. *Eur. Biophys. J.* **2017**, *46*, 325–334. [CrossRef]
39. Man, D.; Mrówka, I.; Wójcik, A.; Pytel, B. Impact of Vanadium(IV)-Oxy Acetylacetonate and Vanadium(III) Acetylacetonatel on the DPPC Liposome Membranes: EPR Studies. *Acta Phys. Pol. A* **2017**, *132*, 52–56. [CrossRef]
40. Białek, M.; Czaja, K. Dichlorovanadium (IV) Complexes with Salen-Type Ligands for Ethylene Polymerization. *J. Polym. Sci. Part A Polym. Chem.* **2008**, *46*, 6940–6949. [CrossRef]
41. Białek, M.; Liboska, O. Vanadium Complex with Tetradentate [O,N,N,O] Ligand Supported on Magnesium Type Carrier for Ethylene Homopolymerization and Copolymerization. *J. Polym. Sci. Part A Polym. Chem.* **2010**, *48*, 471–478. [CrossRef]
42. Białek, M.; Bisz, E. A comparative study on the polymerization of 1-octene promoted by vanadium and titanium complexes supported by phenoxyimine and salen type ligands. *J. Polym. Res.* **2013**, *20*, 164. [CrossRef]
43. Shimshick, E.J.; McConnell, H.M. Lateral phase separation in phospholipid membranes. *Biochemistry* **1973**, *12*, 2351–2360. [CrossRef] [PubMed]
44. Hemminga, M.A. Interpretation of ESR and saturation transfer ESR spectra of spin labeled lipids and membranes. *Chem. Phys. Lipids* **1983**, *32*, 323–383. [CrossRef]
45. Stigter, D.; Mingins, J.; Dill, K.A. Phospholipid interactions in model membrane systems. *Biophys* **1992**, *61*, 1616–1629. [CrossRef]
46. Lawton, J.S.; Aaron, D.S.; Tang, Z.; Zawodzinski, T.A. Qualitative behavior of vanadium ions in Nafion membranes using electron spin resonance. *J. Membr. Sci.* **2013**, *428*, 38–45. [CrossRef]
47. Man, D.; Olchawa, R.; Kubica, K. Membrane fluidity and the surface properties of the lipid bilayer: ESR experiment and computer simulation. *J. Liposome Res.* **2010**, *20*, 211–218. [CrossRef]